Integrated UWB and LIDAR Assisted Localization and Navigation System for Automated Platooning

Tushar Dupga, Ashutosh Deshwal, Sudiksha Navik, Amitangshu Pal
Computer Science and Engineering, Indian Institute of Technology Kanpur, Kanpur, UP, India
Email: {zoro,ashutosh,sudikshanavik,amitangshu}@cse.iitk.ac.in

***Abstract*—Accurate localization and robust navigation are crucial for autonomous robots or vehicles in GPS-denied environments, where traditional methods face signal obstructions and infrastructure limitations. This paper presents an integrated Ultra-Wideband (UWB) based Simultaneous Localization and Mapping (SLAM) framework, implemented on a Robot Operating System (ROS) based Jetbot platform. The system utilizes UWB Time of Flight (ToF) and Angle of Arrival (AoA) for precise localization, along with LiDAR data for real-time mapping and obstacle avoidance. By fusing UWB and LiDAR data, the system tracks a moving target, along with accurate path planning. Experimental results show that the solution achieves a median tracking and navigation error of 18 cm, with 80% of error remains below 20 cm, demonstrating its reliability. This study highlights the feasibility of UWB-based localization for autonomous platooning, offering a scalable and adaptable solution for real-time navigation in dynamic and infrastructure-limited environments.**

***Index Terms*—Automated platooning, Robot navigation, LiDAR-based obstacle avoidance, UWB localization**

I. Introduction

Motivation and background: The rapid advancement of autonomous robotics has brought significant transformations across industries such as logistics, healthcare, and industrial automation. As the demand for autonomous systems capable of navigating in complex environments autonomously grows, challenges arise, particularly in dynamic and signal-deprived conditions. Environments such as mountainous terrains and indoor spaces often pose significant difficulties for localization and path planning, which are critical for the reliable operation of autonomous systems. For example, consider a scenario where a platoon of loaded trucks is moving on a GPS-denied mountainous road, as shown in Fig. 1(a). On the other hand, assume a scenario where a platoon of mobile robots is carrying something in an indoor warehouse without any pre-deployed positioning infrastructure, as shown in Fig. 1(b). In such cases, we assume that the first vehicle/robot is experiencing a controlled navigation (such as manual drivers, or putting more intelligence on the first robot), whereas others are localizing themselves w.r.t. the first vehicle/robot and navigating.

Limitation of the existing techniques: In both scenarios, traditional localization techniques such as GPS, WiFi [1]–[4], RFID [5]–[9], and camera-based systems [10], [11] often face limitations. GPS signals frequently fail in mountainous regions due to obstructions such as hills and valleys. Similarly, camera systems, while useful in open spaces, struggle with issues such as low visibility, obstructions, or sharp turns, making it difficult for the system to reliably track the lead vehicle or robot. Additionally, WiFi and RFID-based systems, though widely used, require extensive infrastructure and are susceptible to signal degradation in non-line-of-sight (NLoS) conditions, further complicating the task of accurate navigation. To summarize, the existing localization methods, while advancing in accuracy and functionality, face several limitations in scenarios requiring minimal hardware and no pre-deployed infrastructure, such as autonomous vehicles/robots assisting each other in dynamic environments like mountains, or indoor warehouses. These limitations highlight the need for more flexible, and robust solutions that can perform reliably without extensive infrastructure setup or high-end hardware.

Our contributions: To address these challenges, Ultra-Wideband (UWB) technology [12]–[15] has emerged as a promising solution due to its ability to deliver precise distance and angular measurements with minimal interference from environmental factors. For example, in the scenario where a platoon of trucks is following closely behind each other on a mountainous road, UWB radios placed on both the leader and following vehicles could exchange distance and angle information. The follower, using the information like time of flight (ToF) and angle of arrival (AoA) data, can determine its position relative to the leader, ensuring that it can maintain its course even in the absence of GPS signals. Similarly, this approach could be applied in indoor environments, such as warehouses, where GPS is unavailable.

While UWB technology offers a reliable means of localization, its integration with other technologies, such as Light Detection and Ranging (LiDAR) sensor, can enhance its effectiveness, particularly for dynamic obstacle avoidance and real-time environmental mapping. LiDAR provides high-resolution spatial mapping, enabling autonomous systems to generate detailed 2D representations of their surroundings. When combined with UWB, which ensures precise localization, this solution allows autonomous systems to better navigate environments filled with dynamic obstacles and complex layouts. The fusion of UWB and LiDAR technologies creates a robust framework for both outdoor and indoor navigation, enabling the system to adapt to changing conditions and provide continuous, accurate navigation. Additionally, the integration of UWB and LiDAR can be further enhanced through the use of Simultaneous Localization and Mapping (SLAM)

This research was supported by the IIT Kanpur Initiation Grant IITK/CS/2021164, and the Research-I Foundation of the Department of Computer Science & Engineering of IIT Kanpur

979-8-3503-9281-4/25/$31.00 ©2025 IEEE

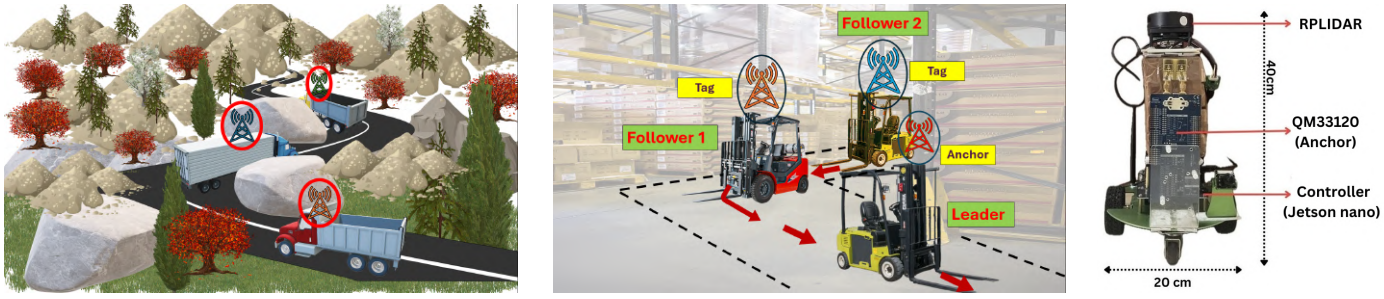

(a) (b) (c)

Fig. 1: An illustration of automated platooning and navigation of (a) vehicles and (b) robots in GPS-denied and infrastructure-less environments. (c) We imitate this scenario using a Jetbot ROS AI Kit along with a UWB radio and Lidar.

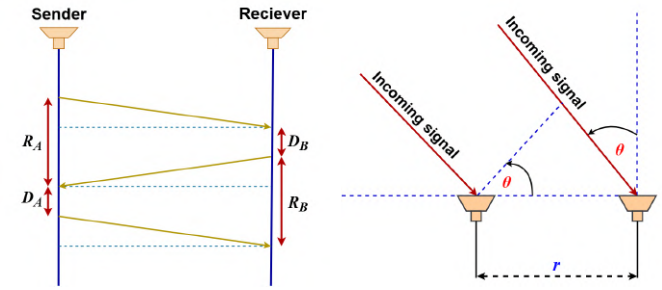

(a) (b)

Fig. 2: Illustration of the (a) TWR, and (b) AoA measurement techniques.

algorithms [16]–[21]. SLAM enables autonomous systems to build accurate maps of their environment while simultaneously localizing their position within the map.

This paper explores the integration of UWB and LiDAR technologies within various SLAM frameworks to assess their performance in indoor and outdoor navigation scenarios. For demonstrating our proposed solution, we build a prototype consisting of a Jetbot ROS kit [22], and integrate an UWB radio on top of it. Through extensive experimentation, we demonstrate that using the proposed scheme, the median navigation error remains within 18 cm, whereas for 80% cases, the error remains below 20 cm. To the best of our knowledge, this is the first work that demonstrates the feasibility of UWB localization on automated platooning, that tries to achieve suitable navigation planning for autonomous systems operating in diverse and challenging environments. A brief demonstration of our proposed solution can be found in https://youtu.be/pmQkcR2vHKI.

Paper organization: The paper is organized as follows. The proposed solution is presented in Section II. Section III outlines the experimental results. Section IV provides an overview of the related literature. The paper is concluded in section V.

II. Proposed Methodology

System architecture: We now discuss the design of the robotic platforms, along with our proposed methodology to implement the automated platooning scheme. The proposed automated system is implemented using the Waveshare Jetbot ROS AI Kit [22], utilizing the NVIDIA Jetson Nano Developer Kit [23] as its central controller. This robust platform is capable of performing advanced robotic tasks, featuring an integrated Inertial Measurement Unit (IMU) [24] that provides precise orientation data for the robot's movements. To drive the robot's mobility, DC motors are used, and controlled through a Proportional Integral Derivative (PID) algorithm [25]. This algorithm ensures smooth, stable, and accurate movement, allowing the robot to navigate through diverse terrains.

For improved navigation and obstacle avoidance, the robot is equipped with a LiDAR [26], [27]. The LiDAR plays a critical role in scanning the environment in real-time, detecting obstacles, and enabling the robot to safely maneuver through its surroundings, making it a vital component for effective navigation. To enable the robot to follow specific objects or paths, it requires a method of localization. For our experiment, we choose the Decawave QM33120WDK1 kit [28], which includes two boards: the QM33120W (anchor) and the QM33110W (tag). This kit allows for highly accurate localization using ToF and AoA measurements.

A key enhancement in this design involves the integration of the QM33120W anchor directly onto the robot's chassis. Additionally, the LiDAR sensor has been elevated to prevent interference with the anchor, ensuring that both sensors function without disruption. This adjustment, illustrated in Fig. 1(c), allows for continuous, accurate LiDAR data collection, which is essential for reliable environmental mapping and obstacle avoidance. The improved configuration ensures that the robot can navigate and determine its position accurately in real-time, maintaining precise control over its movement and understanding of the environment.

ToF and AoA assisted localization: In this study, we utilize an UWB-based localization system to enhance the follower's ability to determine its position accurately w.r.t. the leader and navigate. The QM33120W device, used as an anchor in the localization setup, is equipped with two directional antennas, which are essential for implementing the AoA method. These antennas are spaced at half the wavelength of the UWB signal, i.e. $\frac{\lambda}{2}$, where λ is the signal wavelength. This results in an antenna separation of 1.88 cm, for the UWB frequency of 7987.2 MHz, operating on channel 9. The mobile tag, i.e. the QM33110W board, features a single omnidirectional antenna, allowing it to effectively communicate with the anchor and providing reliable positioning information.

The localization system operates based on the measurement of ToF and AoA in between the leader and followers. For ToF measurement, we use the two-way ranging (TWR) process [29], where the UWB radios exchange three control messages to alleviate the issues related to clock offsets and clock drifts, as shown in Fig. 2(a). From Fig. 2(a), we can observe that the ToF between the devices can be expressed as $\frac{(R_A-D_B)+(R_B-D_A)}{4}$, which is then multiplied with the speed of light to find out the distance between the devices.

In addition to measuring distance, the dual antennas on the QM33120W anchor are utilized to calculate the AoA of the signals received from the UWB tag. By analyzing the phase differences in these signals, the system can determine the angle at which the signal arrives. This enhances the robot's ability to accurately localize itself relative to the target.

The AoA is computed by evaluating the phase shift of the incoming signals across the anchor's antennas. This phase shift provides essential angular information for precise localization. When a signal arrives at an angle θ, it reaches the first antenna before the second, creating a phase difference $\Delta\phi$ based on the distance r between the antennas and the wavelength λ of the UWB signal as illustrated in Fig. 2(b). With these, the phase difference and AoA are calculated as:

$$\Delta\phi = \frac{2\pi r \sin(\theta)}{\lambda} \qquad \Longrightarrow \quad \theta = \arcsin\left(\frac{\Delta\phi \cdot \lambda}{2\pi r}\right)$$

By recalculating the distance and direction to the target in real-time, the system enables the robot to adjust its trajectory efficiently, offering a robust solution for various practical applications.

Dynamic path planning and real-time mapping: The robot's navigation system is implemented utilizing real-time path adjustments, mapping, and tracking. Equipped with LiDAR sensors, the system continuously monitors the environment and detects obstacles in its surroundings. When an obstacle is detected within a 50 cm range, the robot automatically adjusts its path to avoid it, ensuring smooth and safe navigation toward its target, even in unfamiliar or changing environments.

Fig. 3(a)-(b) illustrate two different scenarios of the robot's movement. In Fig. 3(a), the robot follows an unobstructed path towards the tag, with no obstacles on its way. In contrast, Fig. 3(b) presents a scenario in which obstacles are placed between the robot and the tag. Furthermore, Fig. 3(c)-(d) show the environment maps generated by the LiDAR sensors, clearly showing the presence or absence of obstacles.

To enhance the spatial resolution, the robot utilizes SLAM algorithms such as GMapping, Hector SLAM, Cartographer, and Karto SLAM, each offering unique advantages in mapping and localization. GMapping [16]–[18] employs a particle filter-based approach to generate 2D occupancy maps using laser scanners, combined with odometry information for better accuracy. Hector SLAM [19] uses the Gauss-Newton optimization to construct the 2D maps without odometry, making it effective in uneven terrains. Cartographer [20] integrates LiDAR and IMU data to create 2D and 3D maps, improving consistency through loop closure corrections. Karto SLAM [21] focuses

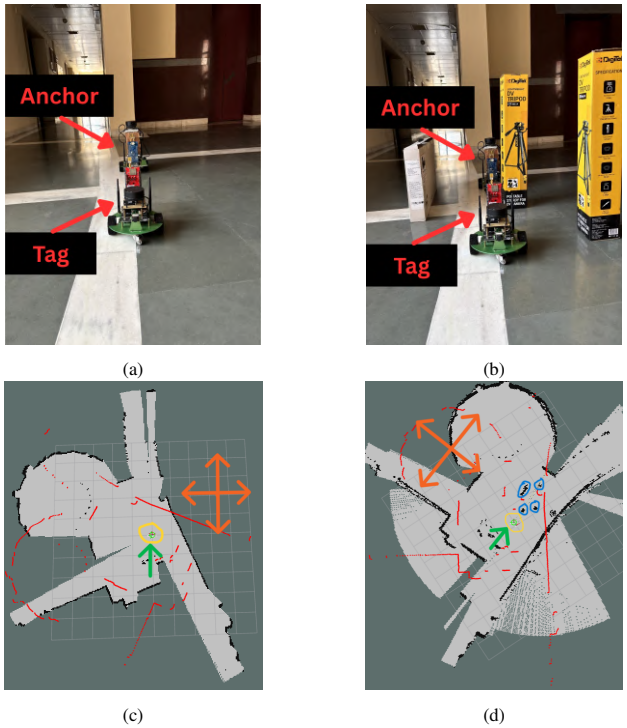

Fig. 3: Robot and tag placed (a) without obstacles and (b) with obstacles in-between, along with their (c)-(d) corresponding LiDAR map. In (c)-(d), the obstacles are marked with blue indicators, whereas the robot is highlighted with a yellow marker and a green pointer indicates its direction of orientation.

on scan matching and sparse posture adjustment, enabling efficient 2D mapping with minimal computational load. By combining these SLAM techniques, the robot continuously updates its environment map, adapting to both known and unmapped areas.

Fig. 4 shows the maps generated by different SLAM algorithms as the robot navigates through the environment. The environment, illustrated in Fig. 4, includes various elements such as cubicles, chairs, and doors. Additionally, individuals were moving within the space during the robot's movement, introducing a dynamic element. Fig. 4(b) clearly demonstrates that the Hector algorithm encounters significant difficulties in mapping its surroundings. As a result, we exclude the Hector algorithm from our further experimental evaluation.

Besides adjusting its path, the robot also uses the localization technique to track the moving target. By frequently updating the target's location, the robot can follow moving objects in real time, making it adaptable to changing environments. Together, the robot's path planning, real-time mapping, and target tracking systems allow it to navigate autonomously and effectively in a wide range of environments.

III. Experimental Evaluation

The experiments are conducted in a controlled environment, where the Jetbot system is tested while navigating through a series of obstacles. To evaluate the performance of the UWB and LIDAR integration, the experiment compares the robots actual path and the ground truth. Additionally, the

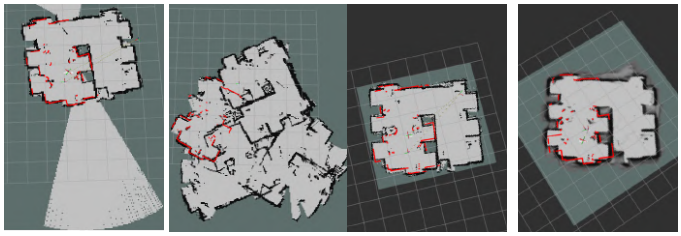

(a) (b) (c) (d)

Fig. 4: Environment map generated using LiDAR and SLAM algorithms (a) GMapping, (b) Hector, (c) Karto, and (d) Cartographer.

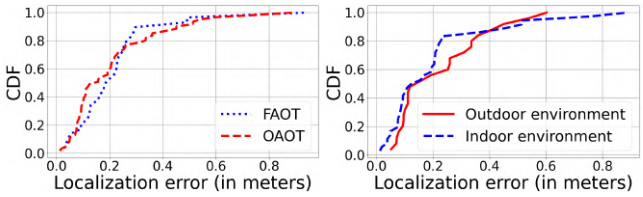

(a) (b)

Fig. 5: (a) Comparison of localization accuracy in FAOT and OAOT scenarios. (b) OAOT localization accuracy across different environments.

robot's ability to avoid collisions and reach its destination successfully is closely studied, providing valuable insights into its navigation capabilities.

UWB-based localization accuracy: We first compare our single-anchor based localization solution using AoA and ToF, with a multi-anchor localization solution using ToF and multilateration, to demonstrate how much the localization error differs. To do this, we examine two localization approaches: a four-anchor one-tag (FAOT) scenario and a one-anchor one-tag (OAOT) scenario, in both indoor and outdoor environments. Testing is conducted under line-of-sight (LoS) and non-line-of-sight (NLoS) conditions, with indoor scenarios including high multipath interference environments such as office cubicles and walls, while outdoor evaluations are performed in open fields and terraces, allowing long-range assessments without obstructions.

From our experiments, we observe that the antenna type significantly influences OAOT localization performance. The omnidirectional tag antenna ensures uniform signal transmission in all directions, whereas the directional anchor antenna enhances the transmission range but is highly susceptible to misalignment, especially when the anchor and the tag are placed almost perpendicular to each other. However, this is not the limitation of the phase difference based AoA measurement, but the limitation of the hardware used. Therefore, to ensure a fair comparison between FAOT and OAOT, the anchor and the tag are placed within $\pm 60^{\circ}$ of each other. Performance evaluation is conducted through 20-25 trials per scenario, covering 0.5 to 6 meters in indoor, and up to 11 meters in outdoor environments.

Fig. 5(a) shows the comparison between OAOT and FAOT. From this figure, we can observe that OAOT performs almost similar to FAOT, while offering greater deployment flexibility, particularly for mobile robot or vehicle navigation. Fig. 5(b) shows the performance of OAOT in different environments. The results demonstrate that the overall localization error remains below 1 meter in both the environments, whereas for 80% of the cases, the error remain below 40 cm. The results also show that OAOT performance remains almost consistent across indoor and outdoor environments, demonstrating its adaptability and usage in general infrastructure-less scenarios.

Comparison of different SLAM algorithms: In this study, we conduct a series of experiments to evaluate the performance of three SLAM algorithms — GMapping, Karto, and Cartographer, across two distinct indoor environments: a cluttered indoor setting and an open indoor space. The cluttered indoor environment, presents a challenging task for the robot navigation, with obstacles such as cubicles, chairs, and moving humans. In contrast, the open indoor environment offers a simpler layout with no obstacles in the robot's path. Each experiment is repeated five times to ensure consistency. During each trial, the robot is given a set of coordinates representing its target positions. The robot then navigates through these target locations, updating its map in real-time while utilizing its LiDAR sensor for object detection and avoidance. The robot continuously refines its map, while navigating.

Fig. 6 compares the navigation accuracy, along with the navigation time using different SLAM algorithms. Fig. 6(a)-(b) show the cumulative distribution function (CDF) of the differences between the robot's actual path with the ground truth for each algorithm. The results reveal significant differences in the algorithm's performance. In the cluttered indoor environment, Karto demonstrates the highest accuracy. GMapping also performs well, but it exhibits slightly higher error rates as compared to Karto. Cartographer, on the other hand, struggles, with a higher overall error, as illustrated in Fig. 6(a). In the open indoor environment, the performance remains consistent. Karto remains the most accurate, while GMapping performance also improves with lower errors. Cartographer, though performing better than in the cluttered setting, still exhibits higher error rate as compared to both Karto and GMapping, as illustrated in Fig. 6(b).

Fig. 6(c) shows the navigation time of the robot using different SLAM algorithms. As observed from this figure, GMapping proves to be the fastest, completing the tasks in $\sim$23 seconds in both the environments. Karto, while slightly slower, strikes a balance between accuracy and speed, taking $\sim$35 seconds in cluttered, and $\sim$24 seconds in open environment. Cartographer is the slowest one, requiring an average of $\sim$77 seconds in cluttered indoor environments, and $\sim$34 seconds in open environment.

Overall, both Karto and GMapping offer good accuracy and speed in both cluttered and open indoor environments. GMapping proves to be the optimal choice for scenarios where speed is critical, while Cartographer, due to its high navigation time and lower accuracy, is less suitable for real-time applications or environments that demand both precision and efficiency. These findings highlight the trade-offs between accuracy and speed, offering valuable insights for selecting the appropriate SLAM algorithm for specific use cases.

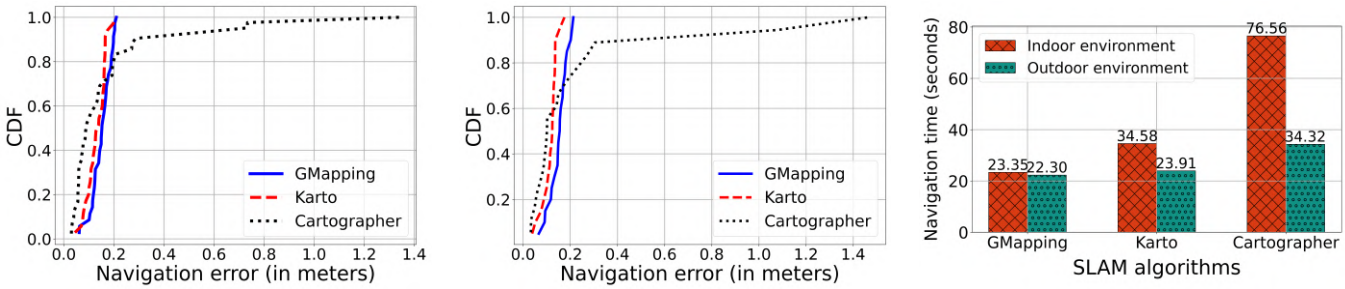

(a) (b) (c)

Fig. 6: Navigation accuracy of different SLAM algorithms in (a) cluttered and (b) open indoor environment. (c) Comparison of the robot's navigation time using various SLAM algorithms.

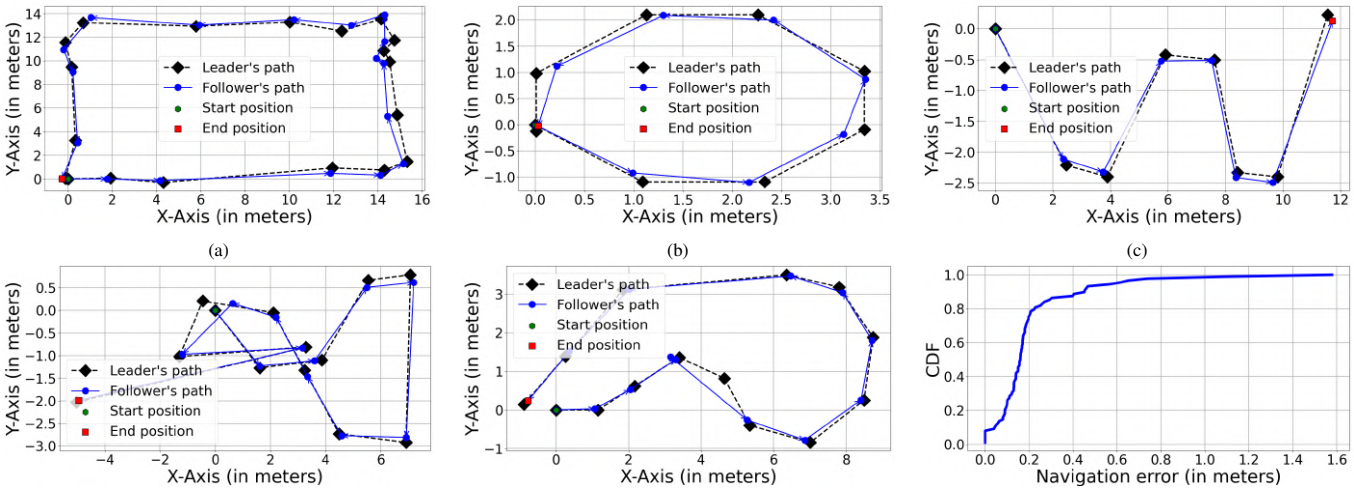

(a) (b) (c) (d) (e) (f)

Fig. 7: (a)-(e) Performance of automated platooning for different navigation trajectories, along with the (f) distribution of navigation errors.

Performance of the integrated localization and navigation scheme: The evaluation of SLAM algorithms demonstrate that while Karto provides the highest accuracy, GMapping offers comparable precision with lower navigation time. Given the need for real-time processing in tracking a moving tag, we choose GMapping as the most suitable approach, and therefore use this for our integrated localization and navigation experiment. For this experiment, we move the leader (with tag) to different positions, and let the follower (having the anchor) follow the leader's trajectory, as shown in Fig. 7. For accurate data collection, the robots remain stationary for 10 seconds, allowing stable data exchange between the anchor and tag using ToF and AoA calculations. Each set comprises of 70 measurements, after which the robot moves to a new position, pauses, and repeats the process.

The robot's tracking performance is evaluated across various indoor environments, as shown in Fig. 7. Fig. 7(a) illustrates its ability to follow a tag along a long corridor, closely aligning with the ground truth trajectory. Additional tests, presented in Fig. 7(b)-(c), position the tag to form geometric shapes like an "octagon" and the letter "W", demonstrating the system's adaptability and precision in maintaining trajectory based on ToF and AoA data. A more dynamic experiment, shown in Fig. 7(d)-(e), introduce some real-world variability by allowing a human to move the tag to different heights and positions. Despite these variations, the robot successfully tracks the tag, confirming the robustness of its localization system in unpredictable environments.

The CDF plot in Fig. 7(f) illustrates the navigation errors between the robot's path and the ground truth. From this figure, we can observe that the median navigation error remains within 18 cm, whereas for 80% of the measurements, the error remains below 20 cm. For all the cases, the error remains within 1.6 meters. Such errors primarily stem from sensor noise, environmental disturbances, and obstacles. Localization challenges arise during sharp turns due to the omnidirectional tag antenna and directional robot antenna. The narrow tag beam reduces angle detection precision, particularly at $\sim 90^{\circ}$ turns, causing minor trajectory deviations. However, even with these restrictions, the tracking remains highly accurate when the tag-anchor angle is less extreme, confirming the system's robustness and reliability.

IV. Related Work

Localization methods span across various technologies, including WiFi, RFID, vision, and UWB systems, each bringing unique strengths and challenges.

RFID-based localization: In [5], the authors have proposed a standalone RFID-based robot navigation method that inte-

grates phase difference data with a particle filter. Authors in [6] have discussed an approach that combines RFID technology with Synthetic Aperture Radar (SAR) and Inverse Synthetic Aperture Radar techniques. In [7], the authors have combined RFID phase difference and readability information to enable centimeter-level localization accuracy even in environments with sparse tags. Further advancements [8] have utilized phase measurements and odometry, ensuring errors below 0.1 meters. Another study in [9] employs SAR with multiple trajectories that effectively reduces localization uncertainty by synthesizing phase data from various paths.

WiFi-based localization: In [1], the authors have developed an autonomous WiFi fingerprinting mechanism for indoor localization. Authors in [2] have proposed a robotic positioning system using multiple WiFi routers. In [3], the authors have developed a deep learning based wireless localization framework with off-the-shelf Wi-Fi devices. A deep fuzzy forest technique is proposed in [4], by combining the merits of decision trees and deep neural networks.

Vision-based localization: Authors in [10] have conducted a comprehensive review of Visual Odometry (VO) and Visual-Inertial Odometry (VIO), and highlighted their effectiveness in GNSS-denied environments. In [11], a modular vision-based system for collaborative robot tasks is introduced, integrating voice command understanding, YOLO-based object localization, and a multi-camera setup with ArUco markers. This system has demonstrated successful human-robot collaboration, showcasing its potential in real-world scenarios.

UWB-based localization: In [12], the authors have introduced a range-focused fusion method that combines monocular cameras, IMU, and UWB technology, improving accuracy while minimizing drift. Building on this, another system [13] has integrated UWB, IMU, and odometer data with adaptive algorithms, excelling in mixed LOS and NLOS environments. In a specialized application, a UWB-based positioning system using an Extended Kalman Filter, combined with IMU data, is employed in [14] for underground coal mining.

V. Conclusion

In this paper, we develop an automated platooning solution that integrates UWB localization, tracking, and SLAM mapping for autonomous navigation across various environments. The system performs well in most scenarios, but challenges arise in complex settings, particularly during sharp turns due to antenna alignment issues. The system demonstrates promising results in tracking a moving tag, though its performance in dynamic environments can be further improved. Future work will focus on refining the system's robustness, particularly in complex scenarios, with additional empirical studies to optimize its performance for a wide range of applications.

References

[1] S. Dai, L. He, and X. Zhang, "Autonomous wifi fingerprinting for indoor localization," 2019. [Online]. Available: https://arxiv.org/abs/1911.11825

[3] R. Ayyalasomayajula *et al.*, "Deep learning based wireless localization for indoor navigation," in *ACM MobiCom*, 2020.

[2] W. Cui, Q. Liu, L. Zhang, H. Wang, X. Lu, and J. Li, "A robust mobile robot indoor positioning system based on wi-fi," *International Journal of Advanced Robotic Systems*, pp. 1–10, 2020.

[4] L. Zhang *et al.*, "Wifi-based indoor robot positioning using deep fuzzy forests," *IEEE Internet of Things Journal*, vol. 7, no. 11, pp. 10 773–10 781, 2020.

[5] H. Wu *et al.*, "A standalone rfid-based mobile robot navigation method using single passive tag," *IEEE Transactions on Automation Science and Engineering*, vol. 18, no. 4, pp. 1529–1537, 2021.

[6] Z. Liu *et al.*, "An isar-sar based localization method using passive uhf rfid system with mobile robotic platform," in *IEEE RFID*, 2020, pp. 1–7.

[7] B. Tao, H. Wu, Z. Gong, Z. Yin, and H. Ding, "An rfid-based mobile robot localization method combining phase difference and readability," *IEEE Transactions on Automation Science and Engineering*, vol. 18, no. 3, pp. 1406–1416, 2021.

[8] A. Tzitzis *et al.*, "Real-time global localization of a mobile robot by exploiting rfid technology," *IEEE Journal of Radio Frequency Identification*, vol. 7, pp. 486–506, 2023.

[9] F. Bernardini, A. O. Cid, and M. St. John, "Robot-based indoor positioning of uhf-rfid tags: The sar method with multiple trajectories," *IEEE Transactions on Instrumentation and Measurement*, vol. 70, pp. 1–15, 2021.

[10] Y. Alkendi, L. Seneviratne, and Y. Zweiri, "State of the art in vision-based localization techniques for autonomous navigation systems," *IEEE Access*, vol. 9, pp. 76 847–76 874, 2021.

[11] C.-C. J. Hsu *et al.*, "Vision-based mobile collaborative robot incorporating a multicamera localization system," *IEEE Sensors Journal*, vol. 23, no. 18, pp. 21 853–21 861, 2023.

[12] T. H. Nguyen *et al.*, "Range-focused fusion of camera-imu-uwb for accurate and drift-reduced localization," *IEEE Robotics and Automation Letters*, vol. 6, no. 2, pp. 1678–1685, 2021.

[13] J. Sun *et al.*, "A novel uwb/imu/odometer-based robot localization system in los/nlos mixed environments," *IEEE Transactions on Instrumentation and Measurement*, vol. 73, pp. 1–13, 2024.

[14] M.-G. Li *et al.*, "Uwb-based localization system aided with inertial sensor for underground coal mine applications," *IEEE Sensors Journal*, vol. 20, no. 12, pp. 6652–6669, 2020.

[15] S. Bhushan, A. Ahluwalia, A. Deshwal, and A. Pal, "Single anchor-based infrastructure-less localization performance using UWB radios," in *DCOSS-IoT*, 2024, pp. 639–646.

[16] G. G *et al.*, "Gmapping: A rao-blackwellized particle filter for grid mapping," 2007, accessed: 2025-02-28. [Online]. Available: https://openslam-org.github.io/gmapping.html

[17] G. G. *et al.*, "Improved techniques for grid mapping with rao-blackwellized particle filters," *IEEE Transactions on Robotics*, vol. 23, no. 1, pp. 34–46, 2007.

[18] G. G., C. Stachniss, and W. Burgard, "Improving grid-based slam with rao-blackwellized particle filters by adaptive proposals and selective resampling," *IEEE ICRA*, pp. 2432–2437, 2005.

[19] S. Kohlbrecher, "Hector mapping," ROS Wiki, 2015, accessed: 2025-03-02. [Online]. Available: http://wiki.ros.org/hector_mapping

[20] T. C. Authors, "Cartographer ros integration," Read the Docs, 2022, accessed: 2025-03-02. [Online]. Available: https://google-cartographer-ros.readthedocs.io/en/latest/

[21] B. Gerkey, "Karto slam," ROS Wiki, 2015, accessed: 2025-03-02. [Online]. Available: http://wiki.ros.org/slam_karto

[22] W. Electronics, "Jetbot ros ai kit," https://www.waveshare.com/wiki/JetBot_ROS_AI_Kit, 2025, accessed: 2025-01-13.

[23] "Get started with jetson nano developer kit," https://developer.nvidia.com/embedded/learn/get-started-jetson-nano-devkit, accessed: 2025-01-13.

[24] Waveshare, "Mpu9250 datasheet," 2025, accessed: 2025-03-08. [Online]. Available: https://www.waveshare.com/wiki/File:MPU9250.PDF

[25] K. H. Ang, G. Chong, and Y. Li, "Pid control system analysis, design, and technology," *IEEE Transactions on Control Systems Technology*, vol. 13, no. 4, pp. 559–576, 2005.

[26] Slamtec, "Slamtec rplidar a1: 360-degree laser scanner," 2025, accessed: 2025-03-08. [Online]. Available: https://www.slamtec.com/en/lidar/a1

[27] Slamtec., "Slamtec rplidar ros package," 2025, accessed: 2025-03-08. [Online]. Available: https://github.com/Slamtec/rplidar_ros

[28] Q. Inc., "Qm33120wdk1 ultra-wideband (uwb) transceiver development kit," https://www.qorvo.com/products/p/QM33120WDK1, 2025, accessed: 2025-01-13.

[29] D. Neirynck, E. Luk, and M. McLaughlin, "An alternative double-sided two-way ranging method," in *WPNC*, 2016, pp. 1–4.